17th World Conference on Earthquake Engineering, 17WCEE
Sendai, Japan - September 13th to 18th 2020

Ductility demand spectra of self-centering structures with the typical flag-shaped hysteretic model subjected to near-fault pulse-type ground motions

H.H. Dong,[1] X.L. Du,[2] Y.L. Zhou, [3] P.F. Li,[4] C. Ma,[5]

[1] *PhD, Key Laboratory of Civil Engineering Safety and Durability of China Education Ministry, Department of Civil Engineering, Tsinghua University, Beijing 100084, China, donghuihui.123@163.com*
[2] *Professor, Key Laboratory of Urban Security and Disaster Engineering of Ministry of Education, Beijing University of Technology, Beijing 100124, China, duxiuli@bjut.edu.cn*
[3] *Research Assistant Professor, Research Institute of Highway Ministry of Transport, Beijing, China, 100088, zhouyulong4554@163.com*
[4] *Research Associate Professor, Research Institute of Highway Ministry of Transport, Beijing, China, 100088, pf.li@rioh.cn*
[5] *PhD, Beijing Advanced Innovation Center for Future Urban Design, Beijing University of Civil Engineering and Architecture, Beijing, 102616, China, machaowater@126.com*

Abstract

Many studies on the ductility demand spectra of structures under near-fault pulse-type ground motions have mainly focused on these structures with the conventional hysteretic models. However, for the self-centering structure with the typically flag-shaped (FS) hysteretic behavior, the corresponding research is limited. The main purpose of this study is to investigate the ductility demand spectra of the self-centering structure with FS model subjected to near-fault pulse-type ground motions based on nonlinear dynamic analyses of single-degree-of-freedom (SDOF) systems. The general features of ductility demand spectra of self-centering structures with the typical flag-shaped hysteretic model are first described. The effects of the structural characteristics on the ductility demand spectra are then systematically studied. This study provides instructive results for the seismic design and retrofitting of the self-centering structure.

Keywords: Ductility demand spectra, near-fault pulse-type ground motions, self-centering structure, FS model, single-degree-of-freedom systems

1. Introduction

Most seismic design provisions allow structures to behave in inelastic state when they are subjected to a strong earthquake ground motion. Many studies indicated that the damage experienced by a structure is closely related to the ductility level, and the ductility factor can be as a performance indicator to estimate structural seismic performance [1-7], in which, the ductility factor is the ratio of the ultimate displacement to the yield displacement of elastic-plastic structures. Therefore, the ductility demand spectrum as an inelastic response spectrum is a useful quantity to design a new structure and estimate existing structural performance and assessing risk [8].

Extensive research works have been carried out to investigate the factors affecting the ductility demands of the structure under earthquakes [9-11]. For example, studies by Ruiz-García and Miranda [12], Medina and Krawinkler [13], and Chopra and Chintanapakdee [2] indicated that the earthquake magnitude and distance to the source have negligible impact on the ductility demand. Hatzigeorgiou [14] pointed out the seismic sequence effect significantly increases the ductility demand for single degree of freedom systems under multiple near-fault and far-fault seismic ground motions. Note also that the impact of different earthquake types on the ductility demand was presented by Hong et al. [15]. It is found that the statistics of displacement ductility demand differs for different earthquake types. Moreover, Goda and Taylor [16] pointed out that the aftershock effects based on the real sequences might underestimate the aftershock impact because of the incompleteness of the real dataset. Besides, several studies also investigated the effects of the hysteretic behavior on the ductility demands [17-23]. At earlier, Lee et al. [24] carried out the statistical studies on ductility demands of five different hysteretic models (elastic-perfectly plastic, bilinear, strength degradation, stiffness degradation and pinching models), the statistical results indicated that the ductility demand is affected by the type of hysteretic model. Vamvatsikos and Cornell [25] developed a probabilistic model of the peak ductility demand based on inelastic SDOF systems with moderate pinching behavior. Goda et al. [26] pointed out that the degradation and pinching effects of the Bouc-Wen model have significant effects on the ductility demand. These research results indicated that the ductility demand is affected by ground motion characteristics and the hysteretic behavior of the structure.

This paper aims to evaluate the ductility demand spectra of self-centering structures with the typical flag-shaped hysteretic model under near-fault pulse-type ground motions based on the nonlinear dynamic analysis of a single degree of freedom (SDOF) system. Here, the target strength reduction factor of the self-centering structure is from 2.0 to 10. The general features of ductility demand spectra of self-centering structures with the typical flag-shaped hysteretic model are first described. Then, the effects of the structural characteristics are then systematically studied. This study provides instructive results for the seismic design and retrofitting of the self-centering structure.

2. Self-centering structures with the typical flag-shaped hysteretic model

The self-centering structure shows the self-centering capability that can return the structure to its initial position after earthquakes. The proposed self-centering structure normally consists of two components, the self-centering component and the energy dissipation component. The self-centering structure can be regarded as the self-centering component and the energy dissipation component assembled in parallel. Fig. 1(a) presents the mass-spring-dashpot idealization of the self-centering structure. In this Figure, Fs and F_E are the forces of the self-centering component and the energy dissipation component, respectively. Because of the self-centering component and the energy dissipations component assembled in parallel, the deformations of the self-centering component and the energy dissipations component are same, and the force of the whole self-centering structure is the summation of those provided by the self-centering component and the energy dissipations component, as shown in Fig. 1(a).

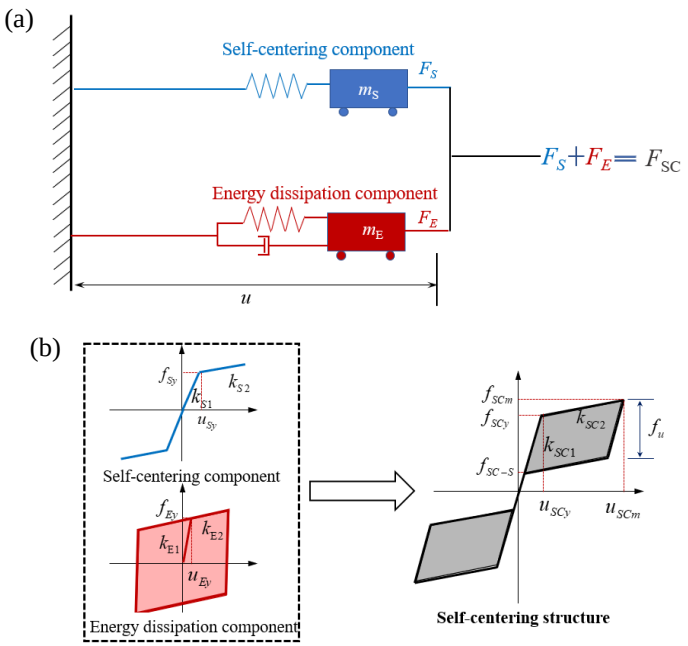

Fig. 1 – Self-centering structure: (a) Mass-spring-dashpot idealization; (b) Simplified hysteretic model

Many studies [27-29] show that the self-centering structure presents the typical FS behavior with the stable energy dissipation ability and the excellent self-centering capability. Fig. 1(b) shows the simplified hysteretic model of the self-centering structure. In which, k_{SC1}, k_{S1} and k_{E1} are the initial stiffness of the whole self-centering structure, the self-centering component and the energy dissipation component, k_{SC2}, k_{S2} and k_{E2} are the post-yielding stiffness of the self-centering structure, the self-centering component and the energy dissipation component, f_{SCy}, f_{Sy} and f_{Ey} are the yield strength of the self-centering structure, the self-centering component and the energy dissipation component, u_{SCy}, u_{Sy} and u_{Ey} are these corresponding yield displacements, f_u is the unloading force, $f_{SC\text{-}S}$ is the self-centering force. The hysteresis response of the self-centering structure equals the superposition of those of the self-centering component and the energy dissipation component.

As shown in Fig. 1(b), several parameters as mentioned above can be used to determine the FS model for the self-centering structure. Two key dimensionless parameters controlling the hysteretic behavior of the self-centering structure are defined in the present study.

(1) Post-yielding stiffness ratio is defined as:

$$\alpha = \frac{k_{SC2}}{k_{SC1}} \tag{1}$$

(2) Energy dissipation ratio of the FS model is given by:

$$\beta = \frac{f_u}{f_{SCy}} \tag{2}$$

where, the energy dissipation ratio controls the energy dissipation capability of the structure, and it also influences the self-centering ability of the structure. The energy dissipation capability becomes better as the energy dissipation ratio increases, whereas, the larger the self-centering force ($f_{SC\text{-}S}$), the smaller the energy dissipation ratio.

The constant-strength ductility demand spectrum is defined as the ratio of the ultimate displacement to the yield displacement of inelastic structures with various vibration periods corresponding to a specific strength reduction factor (R). The displacement ductility factor is defined as:

$$\mu = \frac{u_m}{u_y} \tag{3}$$

where u_m is the maximum demand target displacement of the inelastic SDOF system subjected to the ground motion. The strength reduction factor is defined as the ratio of strength demand of elastic structure to the yield strength of the corresponding inelastic structure under ground motions, which can be expressed as:

$$R = F_e(\mu = 1)/F_y(\mu = \mu_i) \tag{4}$$

where $F_e(\mu=1)$ is the strength demand for an elastic SDOF system (when $\mu=1$), and $F_y(\mu=1)$ is the yield strength of the corresponding inelastic SDOF system with the demand displacement ductility factor (μ) under the earthquake.

3. Selected ground motions

A set near-fault earthquake records with a large long pulse from 26 different earthquake events, which is downloaded from the strong motion database of the Pacific Earthquake Engineering Research (PEER) Center, is selected as shown in Table 1. These motions cover a moment magnitude range from 5.0 to 7.5 and a rupture distance (closest distance from the site to fault rupture plane) range from 0.0 to 19.8 km. The total sample of earthquakes can be characterized as fairly broad since it ranges in terms of shear wave velocity between 163 and 2016 cm/s. The effect of the ground soil condition is not considered for this study, and the mean values for all selected ground motions are used to discuss the analysis results.

Fig. 2 shows the ground acceleration, velocity, displacement and energy flux time history curves of a near-fault pulse-type ground motion (i.e. Rinaldi, 1994 Northridge earthquake). As shown, this ground motion shows a pronounced large long-period pulse in the acceleration history with a similar pulse in the velocity and displacement histories. For this reason, the energy flux sharply increases within a short time range (from 4.5 s to 6.0 s).

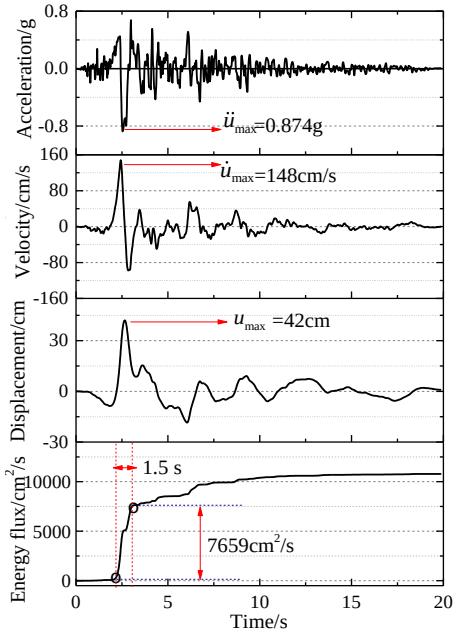

Fig. 2 – Northridge earthquake

Table 1 – Characteristics of selected NF pulse-type ground motion records.

ID	Event	Year	Station	M	Fault distance (km)	V_{s30} (m/s)	PGV (cm/s)
1	San Fernando	1971	Pacoima Dam	6.6	1.8	2016	116.6

2	Coyote Lake	1979	Gilroy Array #6	5.7	3.1	663	51.5
3	Imperial Valley-06	1979	Aeropuerto Mexicali	6.5	0.3	275	44.3
			Agrarias	6.5	0.7	275	54.4
			Brawley Airport	6.5	10.4	209	36.1
			EC County Center FF	6.5	7.3	192	54.5
			EC Meloland Overpass FF	6.5	0.1	186	115
			El Centro Array #10	6.5	6.2	203	46.9
			El Centro Array #11	6.5	12.5	196	41.1
			El Centro Array #3	6.5	12.9	163	41.1
			El Centro Array #4	6.5	7.1	209	77.9
			El Centro Array #5	6.5	4.0	206	91.5
			El Centro Array #6	6.5	1.4	203	111.9
			El Centro Array #7	6.5	0.6	211	108.8
			El Centro Array #8	6.5	3.9	206	48.6
			El Centro Differential Array	6.5	5.1	202	59.6
			Holtville Post Office	6.5	7.7	203	55.1
4	Mammoth Lakes	1980	Long Valley Dam	5.9	18.13	537	43.3
5	Irpinia, Italy-01	1980	Sturno	6.9	10.8	1000	41.5
6	Westmorland	1981	Parachute Test Site	5.9	16.7	349	35.8
7	Coalinga	1983	Oil City	5.8	8.5	389	41.2
			Transmitter Hill	5.8	9.5	477	64.4
			Coalinga-14th & Elm	5.2	10.9	286	36.1
8	Morgan Hill	1984	Coyote Lake Dam	6.2	0.5	597	62.3
			Gilroy Array #6	6.2	9.9	663	35.4
9	N. Palm Springs	1986	North Palm Springs	6.1	4.0	345	73.6
10	San Salvador	1986	Geotech Investig Cent.	5.8	6.3	545	62.3
11	Whittier Narrows	1987	Santa Fe Springs-E.Joslin	6.0	18.5	339	44.3
12	Superstition Hills	1987	Parachute Test Site	6.5	1.0	349	143.9
13	Loma Prieta	1989	Gilroy Array #2	6.9	11.1	271	45.7
			Gilroy Array #3	6.9	12.8	190	44.8
			Saratoga-W Valley Coll.	6.9	9.3	348	62
			Saratoga-Aloha Ave	6.9	8.5	381	53.5
13	Erzican, Turkey	1992	Erzincan	6.7	4.4	275	95.4
14	Cape Mendocino	1992	Petrolia	7.0	8.2	713	82.1
15	landers	1992	Lucerne	5.1	2.2	685	140.3
16	Northridge	1994	Jensen Filter Plant	6.7	5.4	373	67.4
			Jensen Filter Plant Generator	6.7	5.4	526	67.4
			LA Dam	6.7	5.9	629	77.1
			Newhall-W Pico Canyon Rd.	6.7	5.5	286	87.8
			Pacoima Dam (down str)	6.7	7.0	2016	50.4
			Pacoima Dam (upper left)	6.7	7.0	2016	107.1
			Rinaldi Receiving Sta	6.7	6.5	282	148
			Sylmar-Converter Sta	6.7	5.4	251	130.3
			Sylmar-Converter Sta East	6.7	5.2	371	116.6
			Sylmar-Olive View Med FF	6.7	5.3	441	122.7
17	Kobe, Japan	1995	Takarazuka	6.9	0.3	312	72.6
			Takatori	6.9	1.5	256	169.6
18	Kocaeli, Turkey	1999	Gebze	7.5	10.9	792	52
19	Chi-Chi, Taiwan	1999	CHY006	7.4	9.8	438	64.7
			CHY035	7.4	12.7	746	42
			CHY101	7.4	10.0	259	85.4
			TCU036	7.4	19.8	273	62.4

			TCU046	7.4	16.7	466	44
			TCU049	7.4	3.8	487	44.8
			TCU053	7.4	6.0	455	41.9
			TCU054	7.4	5.3	461	60.9
			TCU056	7.4	10.5	273	43.5
			TCU060	7.4	8.5	273	33.7
			TCU065	7.4	0.6	306	127.7
			TCU068	7.4	0.3	487	191.1
			TCU075	7.4	0.9	573	88.4
			TCU076	7.4	2.8	615	63.7
			TCU082	7.4	5.2	473	56.1
			TCU087	7.4	7.0	474	53.7
			TCU101	7.4	2.1	273	68.4
			TCU102	7.4	1.5	714	106.6
			TCU103	7.4	6.1	494	62.2
			TCU104	7.4	12.9	474	31.4
			TCU128	7.4	13.2	600	78.7
			TCU136	7.4	8.3	474	51.8
20	Northwest China-03	1997	Jiashi	6.1	17.7	240	37
21	Chi-Chi, Taiwan-03	1999	CHY024	6.2	19.7	428	33.1
			TCU076		2.7	615	71.2
22	Yountville	2000	Napa Fire Station #3	5.0	0.0	271	43
23	Parkfield-02, CA	2004	Slack Canyon	6.0	3.0	648	53.2
			Parkfield - Cholame 2WA	6.0	3.0	173	57.9
			Parkfield - Fault Zone 1	6.0	2.5	178	81.9
			Parkfield - Fault Zone 12	6.0	2.6	265	56.5
24	Chuetsu-oki	2007	Joetsu Kakizakiku	6.8	11.9	383	91.1
			Yoshikawaku Joetsu City	6.8	16.9	561.6	63.8
			Kashiwazaki City Center	6.8	11.1	294	126
			Kariwa	6.8	12	283	154.5
25	Iwate	2008	IWTH26	6.9	6.0	371	56.9
26	Christchurch, New Zealand	2011	PRPC	6.1	2.0	206	123.1

4. Statistical analyses

The variation trend of the ductility demand spectra of the FS hysteretic model for the self-centering structure is investigated in the present study. The ductility demand spectra are derived through nonlinear dynamic analyses performed by assuming an equivalent viscous damping ratio of 5%. The FS hysteretic model with α =0.05 and β=0.7 is assumed as a target system. Five values of constant strength reduction ratio, namely 2, 4, 6, 8 and 10 are utilized. The natural periods of the structures are set at 50 equi-spaced over 0.1~5.0 s. In order to present the general tendency of the ductility demand spectra, their mean values are calculated for inelastic SDOF systems varying in terms of the period and the strength reduction factor.

4.1 Mean ductility demand spectra

Fig. 3 shows the ductility demand spectra of the FS model for the near-fault pulse-type ground motions. It can be observed that the variation tendency of the ductility demand spectra is first exponentially decreased for the period less than 1.3 s and then converges to a value equal to μ for the period larger than 1.3 s, with the increase of the vibration period. Moreover, it is observed that the ductility demand spectra are very sensitive to the strength reduction factor, and they increase with the increase of the strength reduction factor. The result indicates that a weaker structure (a larger R) corresponds to a larger ductility demand. In this study, the coefficient of variation (COV) is used to evaluate the dispersion of the ductility demand spectra. The COV is defined as the ratio of the standard deviation to the mean value. Fig. 3(b) illustrates the COVs of the ductility

demand spectra of the FS model for the near-fault pulse-type ground motions. As shown, the COVs are approximately strength reduction factor independent. Moreover, the COV is large during the period less than 3.0 s, especially during the period larger less than 0.5 s.

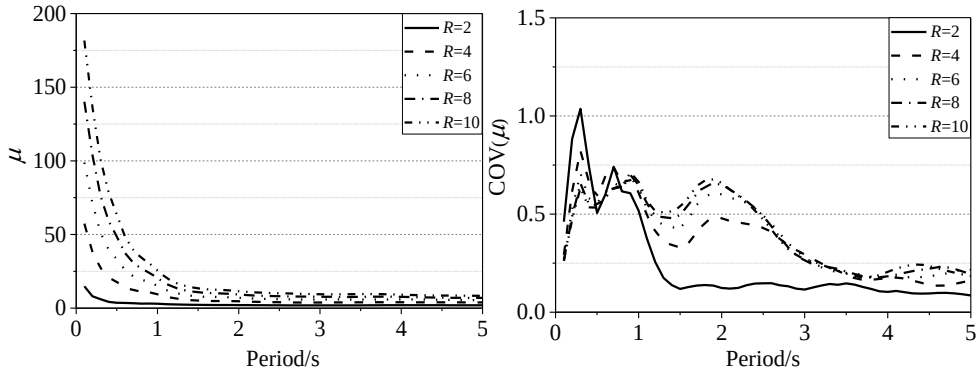

(a) (b)

Fig. 3 – Ductility demand spectra of the FS model (a) mean value, and (b) COVs

4.2 Effect of hysteretic models

To investigate the influence of the FS model on the ductility demand spectra, the Bilinear model and Modified Clough (MC) model are also considered in this section. Fig. 4 presents the three hysteretic models (i.e. FS model, Bilinear model and MC model). Fig. 5 shows the comparisons of the ductility demand spectra for the three models. As shown, the ductility demand spectra for the three models present a similar general trend with the increase of the period and strength reduction factor. It is found that the ductility demand spectra for the FS model are larger than those for the Bilinear model and MC model. For the near-fault pulse-type ground motions, the values of the $\mu_{(i\ model)}/\mu_{(FS\ model)}$ increase first during T<1.0 s and then decrease during 1.0 s≤T<2.5 s and finally tend to be stable during 2.5 s≤T<5.0 s. For the ordinary ground motions, the variation tendency of the $\mu_{(i\ model)}/\mu_{(FS\ model)}$ is to increase during T<0.6 s and tend to be stable during 0.6 s≤T<2.0 s and finally decrease during 2.0 s≤T<5.0 s. Moreover, the values of the $\mu_{(i\ model)}/\mu_{(FS\ model)}$ for the NF pulse-type ground motions and the ordinary ground motions are not both sensitive to the strength reduction factor.

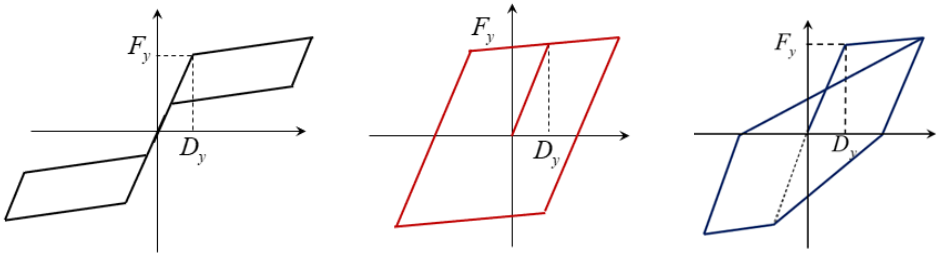

(a) (b) (c)

Fig. 4 – Hysteretic models (a) FS model, (b) Bilinear model, and (c) MC model

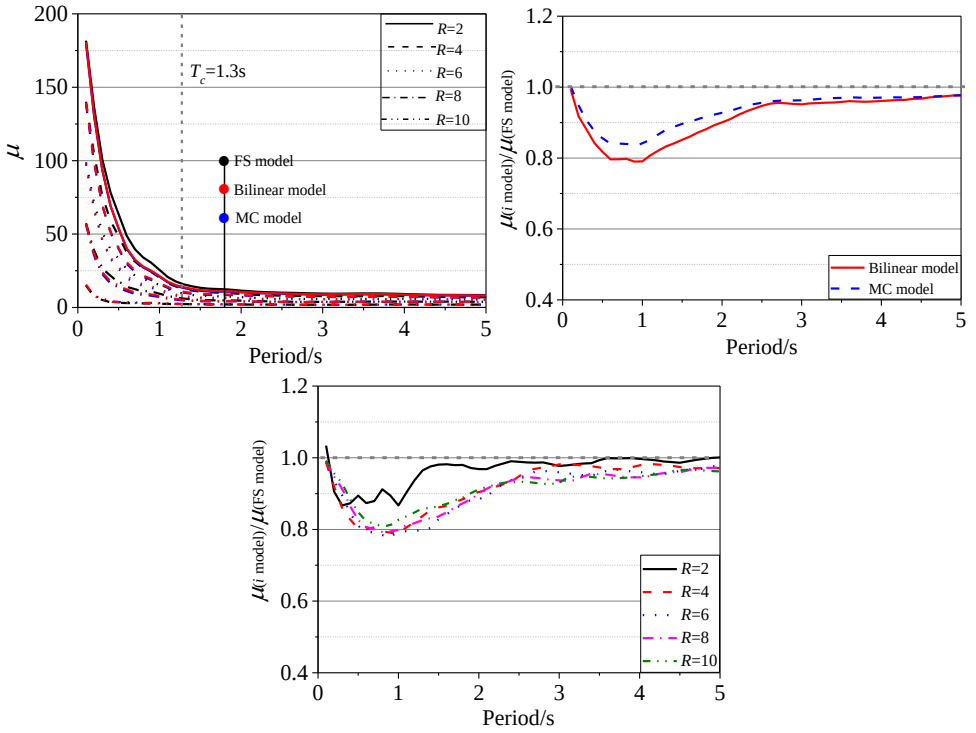

Fig. 5 – Effect of hysteretic models on the ductility demand spectra

4.3 Effect of post-yielding stiffness ratio

In order to investigate the effect of the post-yielding stiffness ratio (α) on the ductility demand spectra of the FS model, the ductility demand spectra for the different strength self-centering structures with α =0.0, 0.05, 0.10, 0.20 and 0.30 are calculated and discussed.

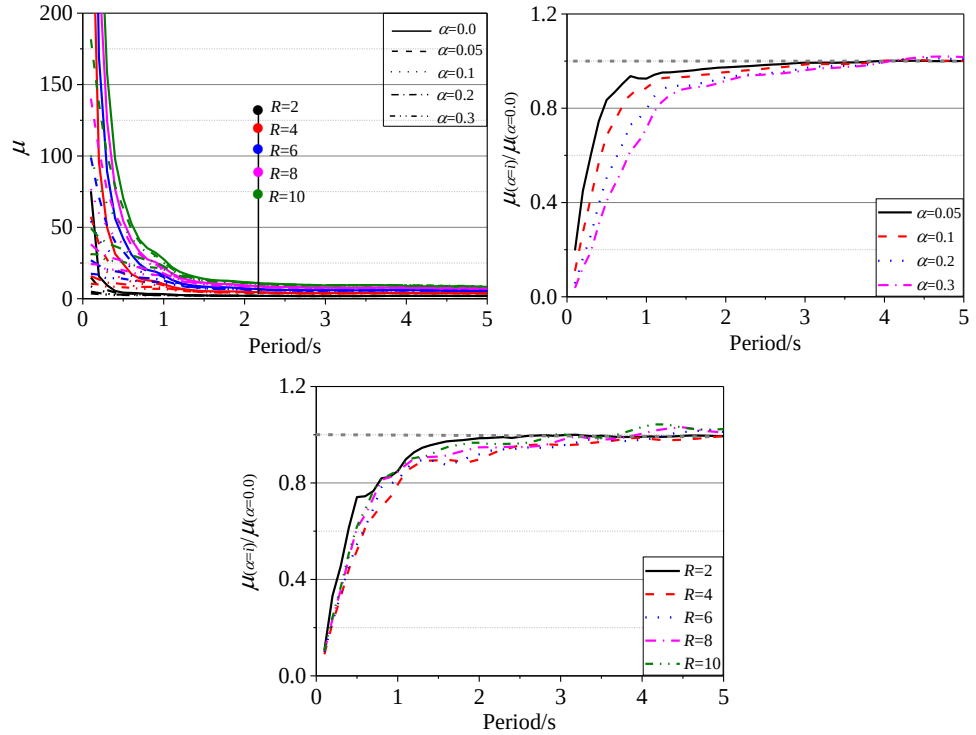

Fig. 6 – Effect of post-yielding stiffness on the ductility demand spectra

The ductility demand spectra of the self-centering structures with α=0.0, 0.05, 0.10, 0.20 and 0.30 are shown in Fig. 6. As shown, the ductility demand spectra for the FS model with various post-yield stiffness ratios present a similar variation tendency. It can be seen that the large post-yielding stiffness ratio significantly induces the small ductility demand spectra during the period less than 1.3 s for near-fault pulse-type ground motions. The ductility demand spectra of the FS model with various post-yield stiffness ratios are almost equal when the vibration period is larger than 1.3 s for near-fault pulse-type ground motions. The result means that the ductility demand for FS model should consider the effect of the post-yielding stiffness ratio.

5. Conclusions

This study assessed ductility demands for SDOF systems under near-fault pulse-type ground motions. A typical FS model is adopted to evaluate the behavior of self-centering systems. The general features of ductility demand spectra of self-centering structures with the typical flag-shaped hysteretic model are first described. Then, the effects of the structural characteristics are then systematically studied. Some conclusions drawn from this study are as follows:

(1) The increase of strength reduction factors always leads to increase in ductility demands and vice versa. Moreover, the ductility demands are extremely dependent on the vibration period of the FS model.

(2) The ductility demand spectra for the FS model are the greatest in three models including the FS model, Bilinear model and MC model.

(3) The post-yielding stiffness ratio has a significant effect on the ductility demands of structures with a vibration period larger than 1.3 s. The larger the post-yielding stiffness ratio, the smallest the ductility demand.

6. Acknowledgements

The authors acknowledge the partial support from the National Key Research Program of China (No. 2017YFE0103000), Postdoctoral Science Foundation of China (2018M641363), Beijing Municipal Education Commission (No. IDHT20190504, KZ202010005001) and the National Science Foundation of China (No. 51908325).

References

[1] Park YJ, Ang AHS, Wen YK (1985): Seismic damage analysis of reinforced concrete buildings. *Journal of Structural Engineering*, **111**(4), 740-757.

[2] Riddell R, Garcia JE, Garces E (2002): Inelastic deformation response of SDOF systems subjected to earthquakes. *Earthquake Engineering & Structural Dynamics*, **31**(3), 515-538.

[3] Chopra AK, Chintanapakdee C (2004): Inelastic deformation ratios for design and evaluation of structures: single-degree-of-freedom bilinear systems. *Journal of Structural Engineering*, **130**(9), 1309-1319.

[4] Akkar SD, Miranda E (2005): Statistical evaluation of approximate methods for estimating maximum deformation demands on existing structures. *Journal of Structural Engineering*, **131**(1), 160-172.

[5] Tothong P, Cornell CA (2006): An empirical ground-motion attenuation relation for inelastic spectral displacement. *Bulletin of the Seismological Society of America*, **96**(6), 2146-2164.

[6] Hong HP, Hong P (2007): Assessment of ductility demand and reliability of bilinear single-degree-of-freedom systems under earthquake loading. *Canadian Journal of Civil Engineering*, **34**(12), 1606-1615.

[7] Yi WJ, Zhang HY, Kunnath SK (2007): Probabilistic constant-strength ductility demand spectra. *Journal of Structural Engineering*, **133**(4), 567-575.

[8] Tena-Colunga A (2001): Displacement ductility demand spectra for the seismic evaluation of structures. *Engineering Structures*, **23**(10), 1319-1330.

[9] Rupakhety R, Sigbjörnsson R (2009): Ground-motion prediction equations (GMPEs) for inelastic displacement and ductility demands of constant-strength SDOF systems. *Bulletin of Earthquake Engineering*, **7**(3), 661-679.

[10] García-Soto AD, Hong HP, Gómez R (2012): Effect of the orientation of records on displacement ductility demand. *Canadian Journal of Civil Engineering*, **39**(4), 362-373.

[11] Yu B, Yang L, Li B (2014): P-Δ effect on probabilistic ductility demand and cumulative dissipated energy of hysteretic system under bidirectional seismic excitations. *Journal of Engineering Mechanics*, **141**(4), 04014141.

[12] Ruiz-García J, Miranda E (2003): Inelastic displacement ratios for evaluation of existing structures. *Earthquake Engineering & Structural Dynamics*, **32**(8), 1237-1258.

[13] Medina RA, Krawinkler H (2004): Seismic demands for nondeteriorating frame structures and their dependence on ground motions. Pacific Earthquake Engineering Research Center. pp. 1381-1381.

[14] Hatzigeorgiou GD (2010): Behavior factors for nonlinear structures subjected to multiple near-fault earthquakes. *Computers & Structures*, **88**(5-6), 309-321.

[15] Hong HP, Garcia-Soto AD, Gomez R (2009): Impact of different earthquake types on the statistics of ductility demand. *Journal of Structural Engineering*, **136**(7), 770-780.

[16] Goda K, Taylor CA (2012): Effects of aftershocks on peak ductility demand due to strong ground motion records from shallow crustal earthquakes. *Earthquake Engineering & Structural Dynamics*, **41**(15), 2311-2330.

[17] Seo CY, Sause R (2005): Ductility demands on self-centering systems under earthquake loading. *ACI Structural Journal*, **102**(2), 275.

[18] Marano GC, Greco R (2006): Damage and ductility demand spectra assessment of hysteretic degrading systems subject to stochastic seismic loads. *Journal of Earthquake Engineering*, **10**(05), 615-640.

[19] Goda K, Hong HP, Lee CS (2009): Probabilistic characteristics of seismic ductility demand of SDOF systems with Bouc-Wen hysteretic behavior. *Journal of Earthquake Engineering*, **13**(5), 600-622.

[20] Lumantarna E, Lam N, Wilson J, Griffith M (2010): Inelastic displacement demand of strength-degraded structures. *Journal of Earthquake Engineering*, **14**(4), 487-511.

[21] Yu B, Yan L, Li B (2014): P-Δ effect on probabilistic ductility demand and cumulative dissipated energy of hysteretic system under bidirectional seismic excitations. *Journal of Engineering Mechanics*, **141**(4), 04014141.

[22] Castaldo P, Palazzo B, Alfano G, Palumbo MF (2018): Seismic reliability-based ductility demand for hardening and softening structures isolated by friction pendulum bearings. *Structural Control and Health Monitoring*, **25**(11), e2256.

[23] Xiang Y, Koetaka Y (2019): Ductility demand of bilinear hysteretic systems with large post-yield stiffness: Spectral model and application in the seismic design of dual-systems. *Engineering Structures*, **187**, 504-517.

[24] Lee LH, Han SW, Oh YH (1999): Determination of ductility factor considering different hysteretic models. *Earthquake Engineering & Structural Dynamics*, **28**(9), 957-977.

[25] Veletsos AS, Newmark NM (1960): Effect of inelastic behavior on the response of simple systems to earthquake motions. Department of Civil Engineering, University of Illinois.

[26] Goda K, Hong HP, Lee CS (2009): Probabilistic characteristics of seismic ductility demand of SDOF

systems with Bouc-Wen hysteretic behavior. *Journal of Earthquake Engineering*, **13**(5), 600-622.

[27] Zhu S, Zhang Y (2007): Seismic behaviour of self-centring braced frame buildings with reusable hysteretic damping brace. *Earthquake Engineering & Structural Dynamics*, **36**(10), 1329-1346.

[28] Dong H, Du X, Han Q, Bi K, Hao H (2019): Hysteretic performance of RC double-column bridge piers with self-centering buckling-restrained braces. *Bulletin of Earthquake Engineering*, **17**(6), 3255-3281.

[29] Erochko J, Christopoulos C, Tremblay R (2014): Design and testing of an enhanced-elongation telescoping self-centering energy-dissipative brace, *Journal of Structural Engineering*, **141**(6), 04014163.

